iJRASET
International Journal For Research in Applied Science and Engineering Technology

INTERNATIONAL JOURNAL FOR RESEARCH

IN APPLIED SCIENCE & ENGINEERING TECHNOLOGY

Volume: 2 **Issue:** XI **Month of publication:** November 2014

DOI:

www.ijraset.com

Call: 08813907089 | E-mail ID: ijraset@gmail.com

International Journal for Research in Applied Science & Engineering Technology (IJRASET)

Review on Aerodynamic Characterization of Wind Turbine under different Flow conditions and drag

Alok Kumar Agrawal[*1], Radheshyam Verma[*2], Sheelesh Kumar Patel[*3],

Prakash Kumar Sen[#4], Shailendra Kumar Bohidar[#5]

[*]*Student, Bachelor of Engg.(Mechanical Engg.) Kirodimal Institute of Technology, Raigarh, Chhattisgarh*
[#]*Faculty, Department of Mechanical Engg. , Kirodimal Institute of Technology, Raigarh, Chhattisgarh*

Abstract - The utilization of wind energy for power generation purpose is becoming increasingly attractive and gaining a great share in the electrical power production market worldwide .Most of the research on wind turbine constitutes condition monitoring and performance optimisation of Vertical axis wind turbine under a constant velocity of air where the transient effect have not been accounted .The non- uniform behaviour of the wind may change the nature of the flow field drag around the VAWT which could decrease its life cycle. This study is an attempt to use Computational Fluid Dynamics techniques to study and analyse the performance of a wind turbine under accelerating and decelerating air inlet velocity .This abrupt change in the instantaneous torque output of the turbine may give rise to highly transient loads on the turbine's structure which may induce heavy stresses on the turbine leading to structural failure .The scope of this study is to investigate the transient response of the turbine under accelerating and decelerating wind flow using CFD and a mathematical model is developed to study the parameter that affect the electrical power generated by the wind turbines. The study shows that the operational aerodynamic parameters has a direct effect on the generated power which will lead the developed and researches to focus on the highest aerodynamic priority that should be considered for manufacturing and suitable the new generation of wind turbines. It has been shown that CFD can be used as an effective tool to predict the performance outputs of a VAWT under varying flow condition.

Keywords- Vertical Axis wind turbine; Computational Fluid Dynamics; Drag; Power Output; turbine performance; Aerodynamics

I. NOMENCLATURE AND SYMBOLS

A	Rotor swept area (m^2)	E,G	Dimensionless factors for axial and tangential interference factors
a, a'	Axial and tangential interference factor		
B	Number of blade		
BET	Blade Element Theory	m_r	Local momentum coefficient for blade station
C	Profile chord for blade (m)		
C_A,C_T	Axial and tangential force factors	n	Number of revolution of rotor per minute(rpm)
C_D, C_L	Drag and lift coefficients		
C_P	Power Coefficient	R	Radius of turbine rotor (m)
Cq	Moment coefficient	r	local radius of turbine rotor (m)
D	Drag force (N)	V	wind speed (m/s)
d	Rotor diameter (m)	V_r	Rated wind speed (m/s)
φ	Aerofoil relative angle	Ω	Angular velocity (rad/s)
η_b	Prandtal Efficiency	α	Angle of attack
ρ	Air density (kg/m3)	λ	Tip Speed Ratio
σ	Solidity	VAWT	Vertical Axis Wind Turbine
λ_d	Design Tip Speed Ratio	HAWT	Horizontal Axis Wind Turbine
λ_r	Local Tip speed Ratio	CFD	Computational Fluid Dynamics

II. INTRODUCTION

The wind is natural phenomenon related to the movement of air passes caused primary by differential solar heating of the earth surface. Wind energy has a great potential to overcome excessive dependents on fossil fuel to meet energy demand. The wind turbine systems can be classified as the horizontal axis turbine(HAWT) and the VAWT based upon the direction the of the axis of rotation. When the wind stream is parallel to the rotational axis of turbine rotor, it is referred to as HAWT.Similarly when the wind direction is perpendicular to the rotational axis of turbine rotor, it is referred to as VAWT Most wind turbine blades where adaptation of airfoils developed for aircraft and were not optimized for wind turbine uses. In recent years developments of improved airfoil section for wind turbines have been ongoing . That may have modifications in order to improve performance for special applications and wind conditions. To gain efficiency , the blade is both tapered and twisted. The taper, twist and airfoil characteristic should all be combined in order to give the best possible energy capture for the rotor speed and site condition[1][2] Milborrrow and Ainsile[3].used a streamline curvature technique for calculation of flow pattern performance prediction. The power coefficient obtained through this method at high rotor loadings were higher than those obtained through momentum considerations. R lanzafame[4]and Messina used the blade element and momentum theory to obtain maximum electrical energy output. Aiming at presenting review on the simulation program that was designed in MAT Lab, in which BET and momentum theories are used to get the formulas that used in this wind control computer program and because the fast running HWAT has chosen therefore the blade number has taken between 1 and 4 aerofoil section NACA 0012.

In India wind power accounts for 6% of India's total installed power capacity, and it generates 1.6% of the country'. A wind turbine is a rotary machine that extracts energy from the wind. There are two forces acting by wind on turbine blades known as Lift and Drag force. The Lift Force is perpendicular to the direction of motion of wind whereas the Drag Force is parallel to the direction of motion of wind. For maximum power generation Lift force should be large and Drag force should be less.

III. POWER COEFFICIENT EVOLUTION

The fraction of power extracted from the power in the wind by a practical wind turbine is usually given the symbol Cp standing for the coefficient of performance which is not a constant, but varies with the wind speed, the rotational speed of the turbine, and turbine blade parameters such as angle of attack and twist angle. The HAWT have variable twist angle, the twist angle is varied to hold power coefficient at it largest possible value up to the rated speed of the turbine, designing the blades to have a maximum coefficient of performance below the rated wind speed helps to maximize the energy production of the turbine.[5]
The axial and tangential interference (a and a') can be calculated from the following relationship

$$8\pi V\beta\Omega(1-a)a'r^2 = W^2C_TC.B \quad \text{.....(1)}$$

Where

$$C_T = C_L\sin\emptyset - C_D\cos\emptyset, C_A = C_L\cos\emptyset + C_D\sin\emptyset$$

From Fig.(1) can get

$$W = \Omega r(1-a')/\cos\emptyset \quad \text{.....(2)}$$

Where the solidity ratio is

$$\sigma = B.\frac{C}{2\pi}.r \quad \text{.....(3)}$$

Substitute equation 2 and 3 in equation 1 can get

$$\frac{a}{1+a} = \frac{r\Omega(1+a)C_TB}{4(\cos\emptyset)^2V(1-a)} \quad \text{.....(4)}$$

From equations 2 and 4 can get

$$\frac{a}{1+a} = \frac{r\Omega(1+a)C_T\sigma}{4(\cos\emptyset)^2 V(1-a)} \left\{\frac{V(1-a)}{\sin\emptyset}\right\} / \left\{\frac{r\Omega(1+a)}{\cos\emptyset}\right\}$$

……(5)

After simplify can get

$$E = \frac{a}{1+a} = \frac{C_T\sigma}{4\sin\emptyset\cos\emptyset} \quad \text{.....(6)}$$

For Fig.(1) can get

$$8\pi V^2(1-a)ar = W^2 C_A CB \quad \text{.....(7)}$$

and

$$W = \frac{V(1-a)}{\sin\emptyset} \quad \text{..... (8)}$$

Substitute equation 8 and 3 in 7 we get

$$G = \frac{a}{1+a} = \frac{C_A\sigma}{4(\sin\emptyset)^2} \quad \text{.....(9)}$$

Tip speed ratio is the dimensionless ratio of the tip speed to the upstream wind speed (V)

$$\lambda = \frac{2R\pi n}{60V} \quad \text{.....(10)}$$

Then From equation 10 and Fig.(1) we get

$$\cot\emptyset = \frac{\lambda\left(\frac{r}{R}\right)(1+a)}{1-a} \quad \text{.....(11)}$$

The torque coefficient is

$$C_q = \frac{2Q}{\rho A V^2 R} \quad \text{.....(12)}$$

But the moment coefficient can get from

$$C_q = 8\int_0^1 \lambda a(1-a)\left(\frac{r}{R}\right)^2 d\left(\frac{r}{R}\right) \quad \text{.....(13)}$$

Substitute equation 11 and 6 in 13 we get

$$C_q = 8\int_0^1 \cot\emptyset\,(1-a)^2 E\left(\frac{r}{R}\right)^2 d\left(\frac{r}{R}\right) \quad \text{.....(14)}$$

Let the local torque coefficient (m_r)

$$m_r = 4(1-a)^2 E\left(\frac{r}{R}\right)^2 \cot\emptyset \quad \text{.....(15)}$$

According to Prandtal, the reduction of efficiency which results is given for wind machine having (B) blades, and the wind rotor

is running in the neighborhood of optimal condition the Prandtal relation follows that

$$\eta_b = [1 - 0.93/B\sqrt{\lambda^2 + 0.445}]^2 \quad \text{.....(16)}$$

Then equation 12 becomes is

$$C_q = 2\int_0^1 m_r \eta_b \, d(\frac{r}{R}) \quad \text{.....(17)}$$

The different values of the coefficient (C_q) as function of (λ) are obtain by measuring the area situated between the various curves graduated tip speed ratio values using numerical integration. Then the power coefficient C_p is related to (C_q) by relation

$$C_p = C_q \lambda \quad \text{.....(18)}$$

IV. ANALYSIS USING CFD

The performance output of a VAWT has been numerically analysed using commercial CFD package (shown fig.(A) & (B)). This VAWT has a diameter of 2m and a height of 1m. The geometry of the VAWT features 12 equally spaced rotor and stator blades respectively. Various flow conditions have been generated in order to analyse the effect of gust of air on the overall performance output of the VAWT. The equations have been solved using iterative method such that each time step corresponds to 3º rotation of the rotor blades the computational model of this turbine consists of 12 rotor and stator blades each as shown in figure 1. The realizable k-ε solver has been used in the following simulations due to its stability during computations and accuracy over a wide range of operating conditions. The sliding mesh technique is used to simulate the rotation of the blades at an angular velocity of 1.143 rad/sec. Second order spatial and temporal schemes have been specified with simple pressure-velocity coupling in the solver. The influx of air into the flow domain is governed by the velocity inlet For the accuracy of the results, the solution needs to be statically steady. It has been observed that during the steady state, model is free from any non-uniformity from 3rd revolution onwards and hence the results are considered after the 3rd revolution only to get an initial converged condition for the transient simulation. During transient analysis, the number of iterations is increased to 100 to allow for convergence.[6][7]

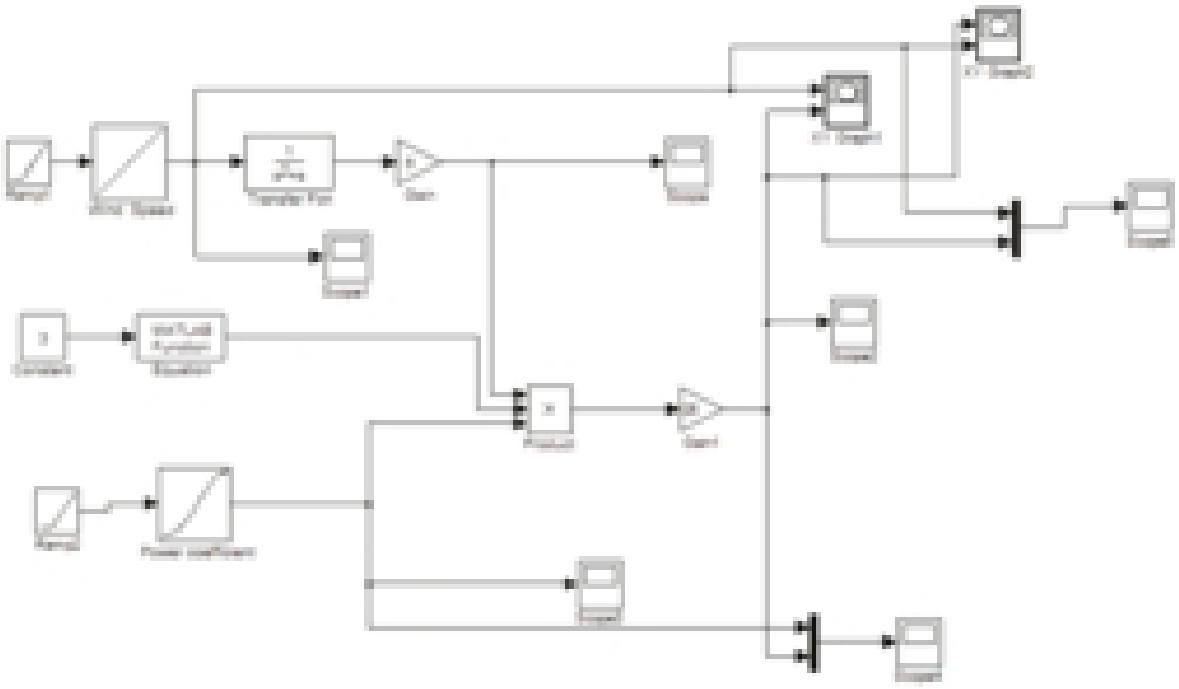

Figure (A) - "Wind control" Computer Program

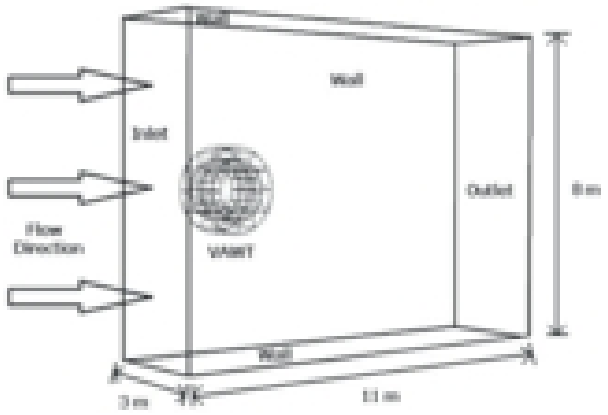

Figure (B) - Flow domain encompassing the VAWT (Courtesy of Google).

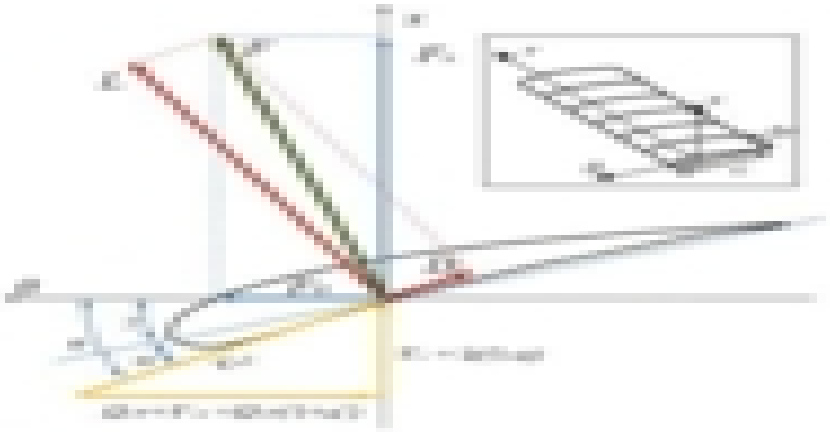

Figure (1). Force & Velocity diagram(Courtesy of Google)

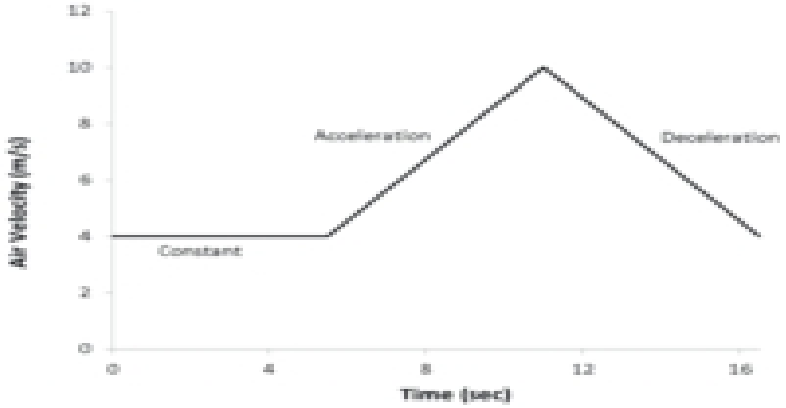

Figure (2) -Change in Inlet Air Velocity with respect to Time.

Condition	Inlet Velocity
1	Constant 4 m/s
2	Accelerating 4m/s to 10 m/s
3	Decelerating 10 m/s to 4 m/s

Table (1)-Different Inlet velocity conditions

A. Flow field Characteristics

Figure (3) shows the velocity contours in the vicinity of the VAWT for both conditions 1 and 2. In this respect, flow field profile can be analysed. It can be seen that the magnitudes of velocity near the stator blades are very small, acknowledging the fact of no-slip boundary condition, however within the stator blade passage, the velocity magnitude represent high values. Furthermore the velocity values under the rotor blades, on the windward side of the turbine, are considerably high. On the rear of the turbine, the velocities are much smaller as compared to the front end. Furthermore, within the rotor blade passages and within the core of turbine, velocity distribution is non uniform. It can be noted the velocity magnitude in case of accelerating condition is considerably high as compared to the normal condition. Furthermore, in accelerated condition, the nature of flow within the central core of the turbine has changed and the shift in the high velocity of jet from the centre towards the leeward side. This jet of air interacts with the rotor blades on the rear end and may affect the torque fluctuation. The figure further reveals the velocity deficit in the wake of the turbine, which may have considerable impact on the downwind turbines when installed in wind farms. In order to further analyse the flow field, pressure contours are shown in figure (4), corresponding to normal and accelerated inlet velocity conditions. Figure depicts highly non-uniform pressure distribution in the turbine region. Specific energy transfer regions corresponding to high pressures can be noted. This high pressure zone is considerably reduced in the wind turbine wake. This pressure drop is due to the energy transfer to the rotor blades. High pressure regions can be seen at the front end of the turbine while low pressures are observed at the rear end. It can be interpreted that the areas of high pressure correspond to low velocities and vice versa. It can further be observed that non-uniform pressure regions exist in the rotor passages and the rotor blades facing the direction of flow, which have maximum contribution to torque output. The high pressure regions above the rotor blades on windward side enhance the rotation of the turbine, thus contributing to increased torque output.

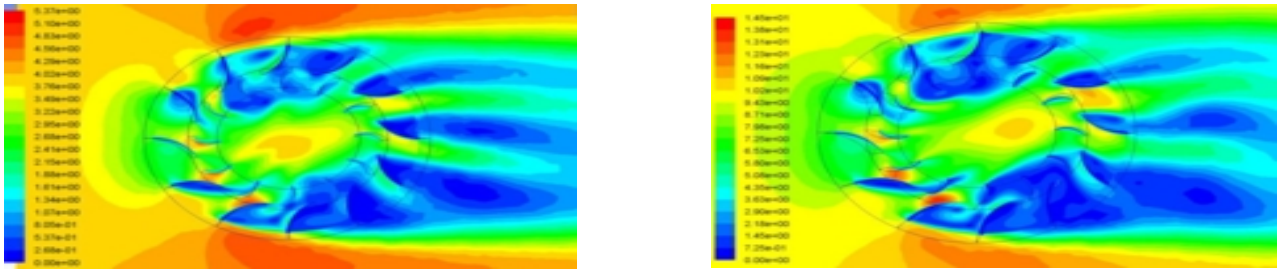

(a) (b)

Figure (3)-Variations in the velocity magnitude in the vicinity of the VAWT during inlet velocity (a) steady at 4m/s (b) transient at peak 10m/s.

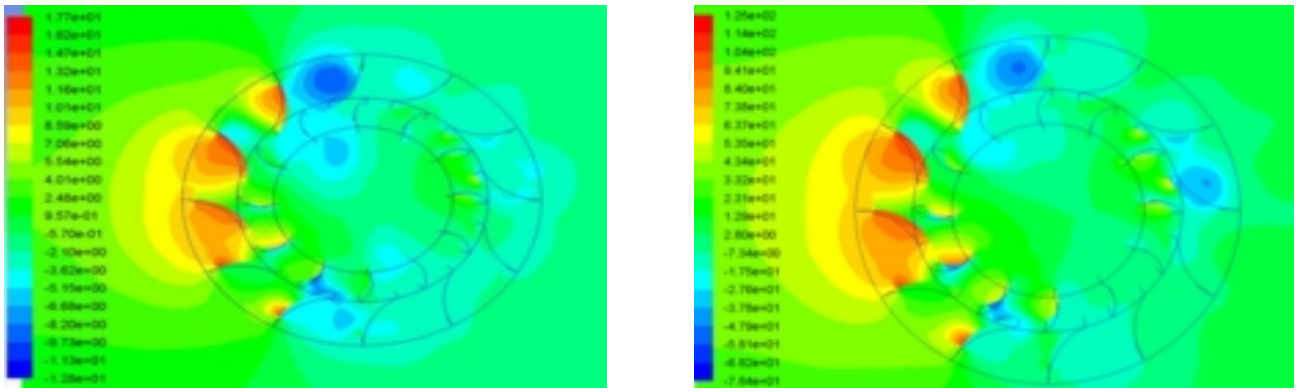

(c) (d)

Fig. 4. Variations in the static pressure in the vicinity of the VAWT during inlet velocity (a) steady at 4m/s (b) transient at peak 10m/s.

B. Performance Characteristics

Figure (5) reveals the values of instantaneous torque output of the turbine during three complete revolutions of the turbine. The angular velocity of the turbine rotor blades is set at a constant value of 1.143rad/s.

During the first revolution i.e. 0-360 degrees, the turbine is running at constant inlet velocity of air at 4m/s and hence the tip speed ratio is constant at a value of 0.2. The torque output in this case has a continuous trend of peaks and valleys. This signature of the torque output corresponds to the angular position of each rotor blade. The peaks are formed when the rotor blade is in line with the stator blade, forming large uniform passages for the flow of air. Whereas valleys correspond to the non-uniform passages in the rotor section due to position of the blade.

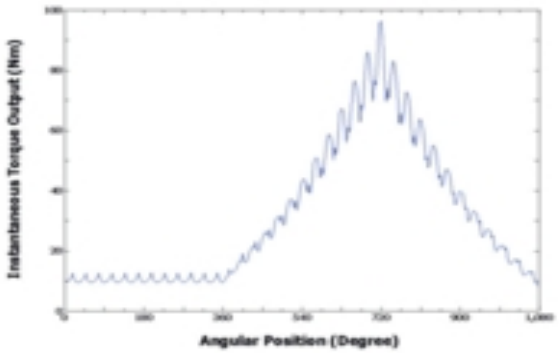

Fig. (5). Instantaneous Torque output from VAWT during normal, accelerating and decelerating flows.

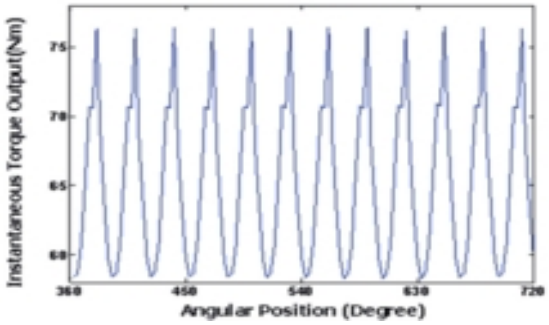

Fig. (6). Instantaneous Torque output from VAWT during steady inlet velocity of 10m/s.

The next revolution of the rotor blades takes place with air inlet velocity changing from 4m/s to 10m/s at an acceleration of 1.09m/s². The continuous upward trend of instantaneous torque output in magnitude can be noted. At 7m/s the torque output averaged for 1m/s increase is 34.4Nm which is 231% higher than the first condition. The maximum torque averaged torque output achieved is 78.2Nm at 10m/s which is 652% higher than that of condition 1 which is due to increase in velocity on the torque output. The cyclic pattern of the torque output also changes, highlighting the effect of transient condition. In order to further analyze the transient behaviour, solution is simulated for a steady inlet velocity of 10m/s as shown in figure (6). It can clearly be seen that in case of constant inlet velocity, the torque output is cyclic and uniform as compared to accelerated condition. Furthermore during acceleration, the maximum torque output achieved is 96.3Nm which is 26% higher as compared to maximum torque at steady state which is 76.5Nm. Similarly the during acceleration, the average torque output obtained is 89.4Nm which is 37% higher as compared to the constant velocity of 10m/s which is 65.2Nm.

The 3rd revolution corresponds to condition when the inlet velocity decelerates from 10m/s to its normal value 4m/s at the rate of 1.09m/s². It is evident from the figure that upon decelerating, there is a trend wise decrease in the torque output with the decrease in the inlet velocity. The cyclic pattern of the torque also changes during initial acceleration and during last few cycles of deceleration. The blade position with respect to peak and pits changes during acceleration and deceleration as compared to the steady inlet velocity condition. This can be illustrated in figure (7).

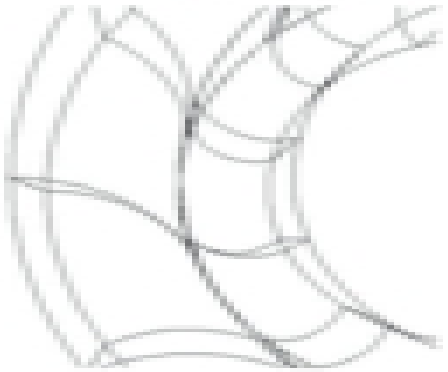

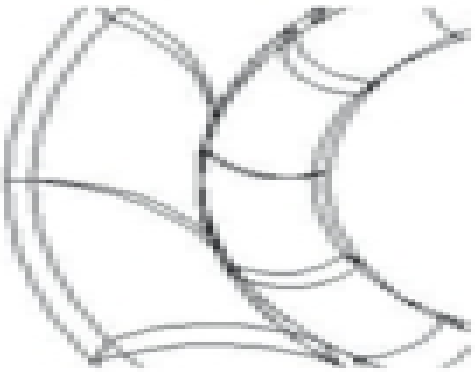

(a) *(b)*

Fig. (7). Blade Position during Pit (a) Accelerating after 8m/s Instantaneous, (b) Decelerating after 5m/s.

The torque signatures formed in the accelerating condition are not only non-conforming to the ones during steady inlet velocity of 10m/s but an interesting factor to note is that they are also non-conforming to decelerating torque signatures. These different torque signatures highlight the fact of transient conditions with continuously changing TSRs on the torque output. To show the performance characteristics of the turbine, both average torque and power output values can be plotted against the transient velocity of air in figure (8). TSR is plotted on a separate axis for reference.

Figure (8) shows the values of torque and power outputs, based on each 1m/s averaging period during acceleration and deceleration. It is observed that the TSR decreases as the inlet velocity increases for accelerating flow. Furthermore, the TSR increases as the flow velocity increases for decelerating flow. The figure also reveals that during accelerating air velocity, as the TSR decreases, the torque output and the power output of the turbine increases. The maximum average power output achieved is 89.4W with the instantaneous torque value of 78.2Nm; which are considerable high as compared to power and torque output values during constant velocity of 4m/s air inlet velocity power and torque output values which are 11.8W and 10.4Nm respectively.

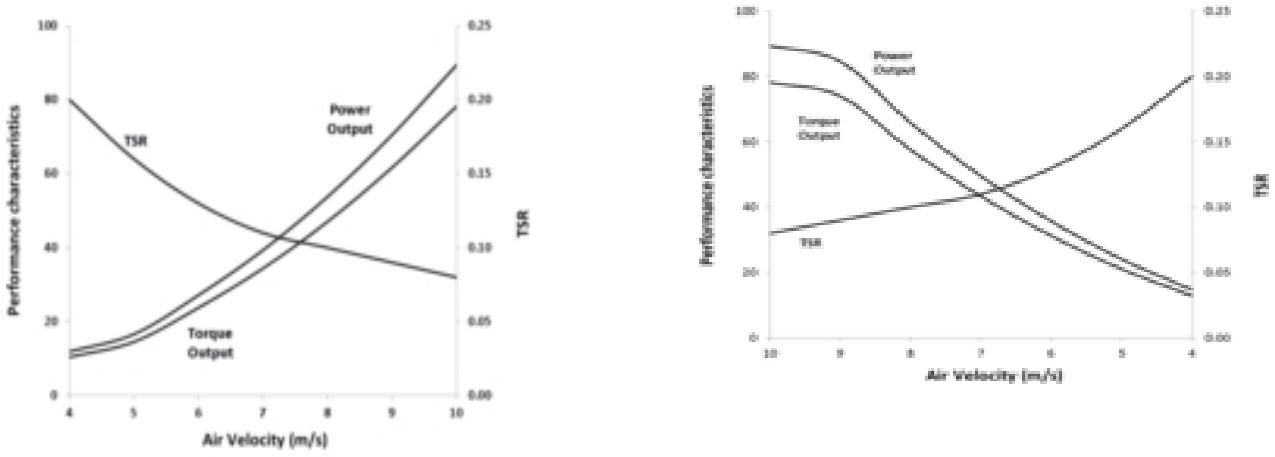

(a) (b)

Fig. (8). Performance characterizes of the VAWT during changing velocity (a) Accelerating, (b) Decelerating.

At the start of deceleration, power output achieved is high, which shows downward trend as the inlet velocity changes gradually to 4m/s. It can be noted that there is a steep reduction in power output as compared to the reduction in power output at the start of deceleration. This can be further summarized in Table 2 that presents the average torque/power output for each m/s change in velocity. It can be seen that the average torque and power outputs increase for accelerating flows whereas the torque and power outputs decrease for decelerating flows.

.

Accelerating			Decelerating		
Velocity m/s	Torque Output	Power Output	Torque Output	Power Output	%Difference in Power output
4-5	14.52	16.60	12.95	14.80	10.82
5-6	23.76	27.16	21.12	24.12	11.19
6-7	37.40	39.32	31.24	35.71	9.18
7-8	47.03	53.76	43.34	49.54	7.84
8-9	61.65	70.45	57.57	65.80	6.62
9-10	78.20	89.38	73.95	84.52	5.44

Table 2. Average Torque/Power Output during each m/s increase in velocity

This validates the phenomena that increase in the velocity of the air significantly increases the power output from the turbine. Furthermore, it can be observed that during change in velocity from 4m/s to 5m/s, the power output during accelerating condition is 16.6W while during decelerating condition the power output during the same velocity change is14.8W hence giving a difference of 11%. During the first complete revolution the average torque output obtained from the turbine is 12.6Nm, during

the accelerating flow, the values of average torque output achieved is 43.2Nm while during the decelerating flow of air the average torque output, given by the turbine during whole revolution, is 40Nm. However this percentage difference increases during change of velocity between 5m/s and 6m/s, and then decreases giving the percentage difference between acceleration and deceleration between 9m/s and 10m/s as 5%.In this regard, this percentage difference between accelerating and decelerating values doesn't show any clear trend. Hence, in order to quantify the results, further analysis of the torque signatures is carried out. Table 3 depicts the maximum torque and the peak to peak amplitude of the torque.

Air Inlet Velocity	T_{max}	Peak to Peak Amplitude	% Difference w.r.t. Normal
4	12.64	3.04	
5	18.91	4.32	42.11
6	29.93	5.90	94.08
7	43.12	9.65	217.43
8	58.62	14.10	363.82
9	76.50	20.50	574.34
10	96.28	26.65	776.64

(a) Accelerating

Air Inlet velocity	T_{max}	Peak to Peak Amplitude	% Difference w.r.t. Normal
10	96.28	26.65	776.64
9	80.12	18.18	498.03
8	62.33	14.70	383.55
7	46.55	11.14	266.45
6	33.14	8.57	181.91
5	21.91	6.32	107.89
4	13.23	4.73	55.59

(b)Decelerating

Table 3. Peak to Peak Amplitude for the Torque Outputs.

The torque output from the turbine reveals another aspect. It can be seen that as the air inlet speed increases, the peak to peak amplitude of torque output also increases. This variation is recorded as 3.04Nm as maximum in case of inlet velocity of air at 4m/s. When the inlet velocity of air accelerated to 10m/s, the peak torque output achieved is 96.3Nm and the maximum peak to peak amplitude of torque is recorded as 26.6Nm which is 776% high as compared to the constant velocity condition. These high fluctuations in torque output may give rise to highly transient loads on the turbine's structure which may induce heavy stresses on the turbine leading to structural failure. Same analysis implies to decelerating condition, where the variation in torque amplitude decreases as the velocity decreases. The peak to peak amplitude is highest at high inlet velocity and then this decrease with the change in velocity and further reduces to 4.7Nm for inlet velocity of 4m/s. Here it highlights the fact that although the velocity has resumed to its original value of 4m/s, still there is the difference between peak to peak amplitude between steady state and the transient state which is 55%. It implies that the turbine will take some time to revert back to its normal average torque production.

C. AIR DRAG CHARACTERISTICS

The definition of the drag coefficient for wind turbine blade is based not on the frontal area but on the plan area, for reasons that will become clear later. The flow past a body which has a large span normal to the flow direction is basically two-dimensional and in such cases the drag coefficient can be based upon the drag force per unit span using the stream-wise chord length for the definition.[10]

$$C_D = \frac{Drag/\,unit\ span}{0.5 * \rho * u^2 c}$$

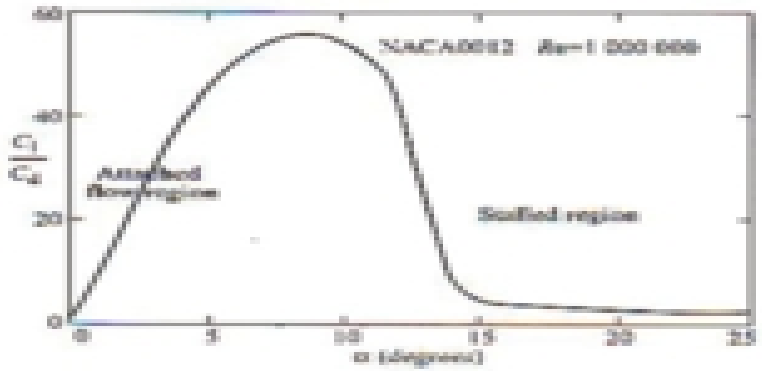

Figure (9). The Pressure distribution around aerofoil NACA0012

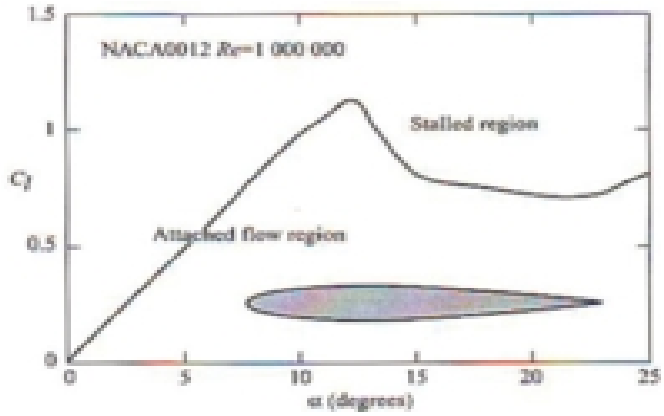

Figure (10). Lift/Drag ratio variation

For a wing of large span the value of CD is roughly 0.01, at moderate Reynolds number. The drag coefficient of an aerofoil also varies with angle of attack. Fig.(9) shows that on the upper surface pressure is rising as the flow moves towards the trailing edge, this is called an adverse pressure gradient and seeks to slow the air down. If the air is slowed to a standstill stall will occur and the pressure drag will rise sharply. The strength of the adverse pressure gradient increases with angle of attack and so it can be expected that the drag will rise with angle of attack. Figure (9) shows the variation of C_D with α also for the symmetrical NACA0012 aerofoil. The lift/drag ratio{shown in Fig. (10)} has a significant effect upon the efficiency of a wind turbine and it is desirable that a turbine blade operates at the maximum ratio. The nature of the flow pattern around an aerofoil is determined by the Reynolds number and this significantly affects the values of the lift and drag coefficient. The general level of the drag coefficient increase with decreasing Reynolds number and below a critical Reynolds number of about 200000 the boundary layer remains laminar causing a sharp rise in the coefficient. The affect on the lift coefficient is largely concerned with the angle of attack at which stall occurs. As the Reynolds number rises so does the stall angle and because the lift coefficient increases linearly with angle of attack below the stall, the maximum value of the lift coefficient also rises. Characteristic for the NACA0012 aerofoil are shown in Fig.(11).

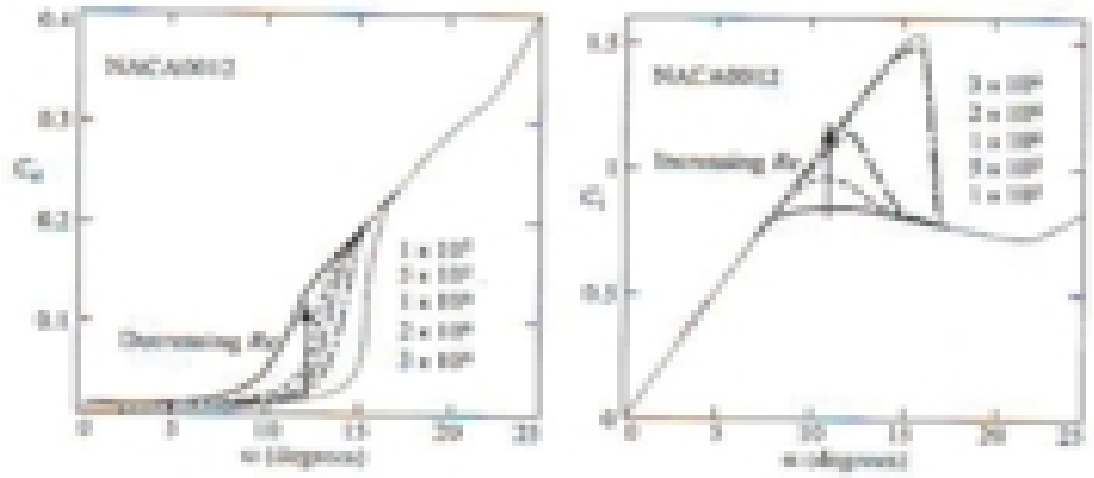

Figure(11). Variation of the drag and lift coefficient with Reynolds Number in the stall.

1. Figure (12) the Cp-λ performance the first point to notice is that maximum value of Cp is only 0.47, achieved at tip speed ratio of 7, which is much less than Betz limit. The discrepancy is caused in this case by drag & tip losses but the stalls also reduce the Cp at low value of the tip speed.

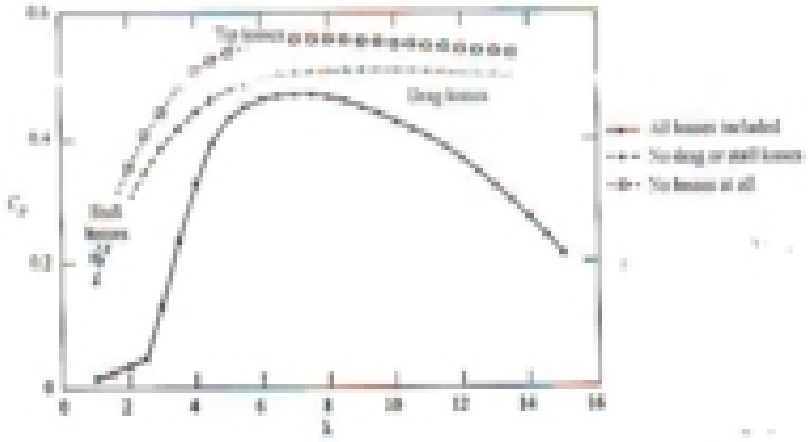

Figure (12). Performance curve for three blade turbine

2. The other principle to consider is the solidity. For the three blade machine above the solidity is 0.0345 but this can be altered by changing its number of blades The main effect to observe of changing solidity are as follows, see Fig.(14). Low solidity produce a board, flat curve which means that the CP will change very little over a wide tip speed ratio range but the maximum CP because the drag losses air high. High solidity produced a narrow performance curve with a sharp peak making the turbine very sensitive to tip speed ratio changes and if solidity is too high, has a relatively low maximum CP. the reduction in CPmax is caused by stall losses. An suitable solidity appears to be achieved with three blades, but two blades might be an acceptable alternative because although the maximum CP is a little lower the spread of the peak is wider and that might result in a larger energy capture. It might be argued that a good solution would be to have a large number of blades of small individual solidity but this greatly increases production costs and results in blades which are structurally weak and very flexible.
3. Fig.(13) shows how the torque developed by a turbine rises with increasing solidity. For high speed turbines designed for electricity generation as low a torque as possible is desirable in order to reduce gearbox costs. The peak of the torque curve occurs at a lower tip speed ratio than peak of the power curve. The peak of curve occurs while the blade is stalled.
4. Fig.(15) the effect of solidity on thrust, the thrust force on the rotor is directly applied to the tower on which the rotor is supported and so consideration influences the structure design of the tower. The thrust on the rotor are increases with increasing solidity.

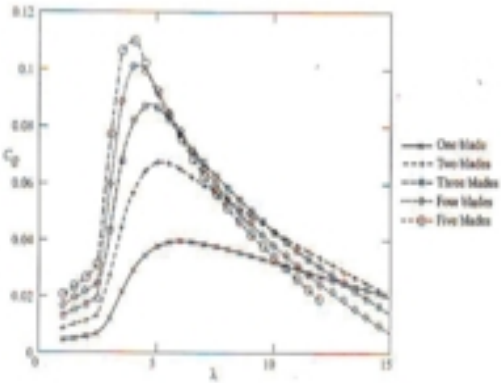

Figure(13). Effect of changing of Solidity

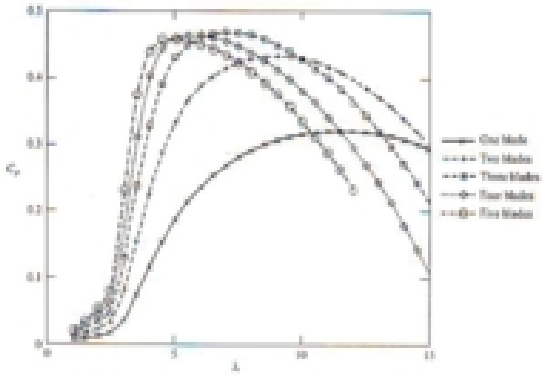

Figure(14). The effect of Solidity on torque

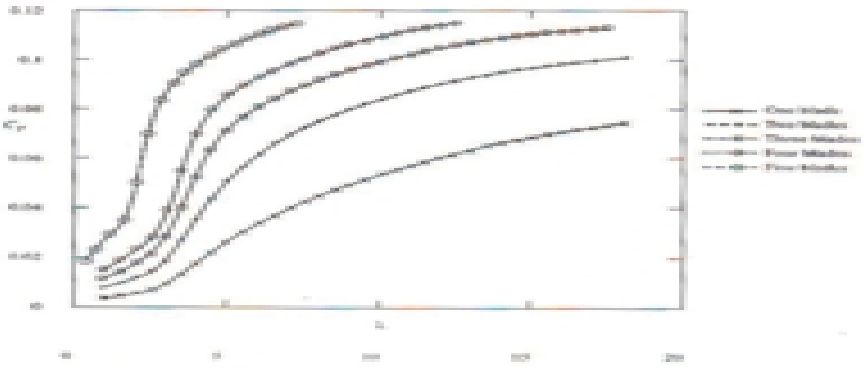

Figure (15).Effect of solidity on Thrust.

V. CONCLUSION

With the help of CFD analysis it can be concluded that number of stator and rotor blades, and their combination, affects the performance output of Vertical Axis Wind Turbines. It has been concluded that increase in the number of rotor blades increases the torque output from VAWT. It has also been observed that VAWTs having same number of rotor and stator blades yield highest power. The interaction of the rotor and stator blades generates a complex flow field characterised by increase in pressure at the interface between the rotor and the stator blades. The comparison of curved and straight stator blades show that curved stator blades generates higher power and delays the onset of churning in VAWTs. It has also been observed that Computational Fluid Dynamics based techniques are capable of capturing the complex flow phenomenon in the vicinity of VAWTs with reasonable accuracy and hence can be used as tool for analysing VAWT's performance. It has also been shown that CFD can be used as an effective tool to predict the performance outputs of a VAWT under varying flow conditions and total life cycle of the VAWT can be computed. Future work could extend this study and modelling of the VAWT. This is fundamental for the future improvement of the VAWT.

REFERENCES

[1] G.D.Rai, Non Conventional Energy Sources, Wind energy, pp. 242- 270, Khanna Publication, fifth edition: 2011,Apr. .
[2] Andres Ahlstrom,"Aeroelastic Simulation of Wind Turbine Dynamics",PhD thesis from Royal institute of technology Department of Mechanics, Sweeden April 2005.
[3] Milborrow,D.J and Anslie,J.F."Calculation of Flow Patters and Performance of wind Turbine using streamline Curvature Method"proc.Second BWEA Wind Energy Workshop, Cranfield 1980.
[4] R Lanzafame and Messina "Optimal wind turbine design to maximize energy production "Proc.IMechE volume 223 part A:J.Power and Energy,Italy 2008.
[5] Dr.Eng.Ali H.Almukhtar, "Effect of Drag on the performance for an efficient wind turbine blade design", Science direct, Elsevier Ltd.,Energy Procedia 18 (2012) pp.404-415.
[6] Atif Shahzad,Taimoor Asim, Rakesh Mishra, Achilleos Paris-"Performance of a vertical axis wind turbine under Accelerating and Decelerating Flows", Science Direct, Elsevier Ltd., Procedia CIRP 11(2013) pp.311-316.
[7] Rosario Nobile, Maria Vahdati, Janet F.Barlow, Anthony Mewburn-Crook-"Unsteady flow simulation of a vertical axis augmented wind turbine: A two dimensional study ,J.Wind Eng.Ind.Aerodyn.125(2014) pp.168-179.
[6] Colley, G. and Mishra, R. Computational flow field analysis of a Vertical Axis Wind Turbine, In proceedings of the International Conference on Renewable Energies Power Quality, Las Palmas, Gran Canaria (2011).
[7] Colley, G. and Mishra, R. Effect of rotor blade position on Vertical Axis Wind Turbine performance, In proceedings of the International Conference on Renewable Energies and Power Quality (ICREPQ'10) Granada, Spain (2010).
[8] Manwell, J.F. Mcgowan, J.G. and Rogers, A.L.Wind Energy explained: Theory, Design and Application(2009); 2nd Ed., John Wiley & Sons Ltd., Chichester, UK.
[9] Park, K.S. Asim, T. and Mishra, R. Computational Fluid Dynamics based fault simulations of a Vertical Axis Wind Turbine, Journal of Physics: Conference Series (2012); 364.
[10] R.K.Bansal, Fluid Mechanics and Hydraulic Machines, Air Drag coefficiet,2013
[11] Huimin Wang, Jianliang Wang, Ji Yao, Weibin Yuan, Liang Cao-"Analysis on the aerodynamic performance of vertical axis wind turbine subjected to the change of wind velocity"Science Direct, Elsevier Ltd., Procedia Engineering 31(2012)pp.213-219.

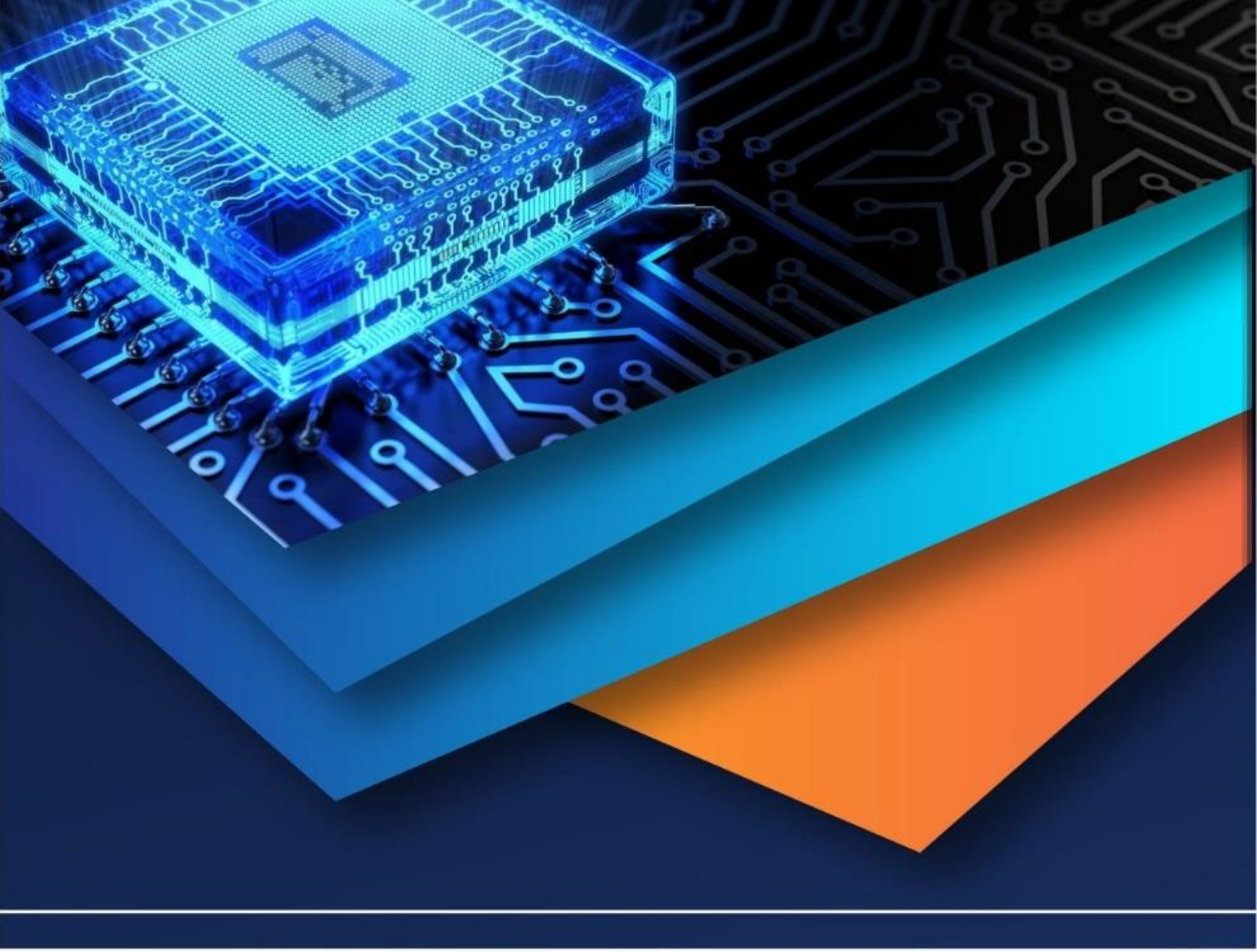

10.22214/IJRASET

45.98

IMPACT FACTOR: 7.129

IMPACT FACTOR: 7.429

INTERNATIONAL JOURNAL FOR RESEARCH

IN APPLIED SCIENCE & ENGINEERING TECHNOLOGY